C. R. Geoscience 348 (2016) 52–60

Contents lists available at ScienceDirect

Comptes Rendus Geoscience

www.sciencedirect.com

Tectonics, Tectonophysics

Off-fault tip splay networks: A genetic and generic property of faults indicative of their long-term propagation

Clément Perrin [a], Isabelle Manighetti [a,*], Yves Gaudemer [b]

[a] Université Nice Sophia-Antipolis, CNRS, IRD, Observatoire de la Côte d'Azur, Geoazur UMR 7329, 250, rue Albert-Einstein, Sophia-Antipolis, 06560 Valbonne, France
[b] Institut de physique du globe de Paris, Sorbonne Paris Cité, Université Paris-Diderot, CNRS, 75005 Paris, France

ARTICLE INFO

Article history:
Received 25 March 2015
Accepted after revision 18 May 2015
Available online 3 July 2015

Handled by Vincent Courtillot

Keywords:
Faults
Splays
Propagation
Stress
Damage

ABSTRACT

We use fault maps and fault propagation evidences available in the literature to examine geometrical relations between parent faults and off-fault splays. The population includes 47 worldwide crustal faults with lengths from millimetres to thousands of kilometres and of different slip modes. We show that fault splays form adjacent to any propagating fault tip, whereas they are absent at non-propagating fault ends. Independent of fault length, slip mode, context, etc., tip splay networks have a similar fan shape widening in direction of long-term propagation, a similar relative length and width (~30 and ~10% of parent fault length, respectively), and a similar range of mean angles to parent fault (10–20°). We infer that tip splay networks are a genetic and a generic property of faults indicative of their long-term propagation. Their generic geometrical properties suggest they result from generic off-fault stress distribution at propagating fault ends.

1. Introduction

All faults grow larger in time as they accommodate more strain (with exception of subduction faults; e.g., Cowie and Scholz, 1992a,b; d'Alessio and Martel, 2004; Manighetti et al., 2001a; Nicol et al., 2005; Segall and Pollard, 1983). The growth of faults has been observed in natural cases (e.g., Armijo et al., 1999; Childs et al., 2003; Jackson et al., 1996; Keller et al., 1999; Manighetti et al., 1997, 1998, 2001b), inferred from scaling relations between fault length and accumulated displacement (e.g., Cartwright et al., 1995; Cowie and Scholz, 1992a; Dawers et al., 1993; Manighetti et al., 2001a; Marrett and Allmendinger, 1990; Schlische et al., 1996; Walsh and Watterson, 1988), and modeled experimentally (e.g., Mansfield and Cartwright, 2001; Otsuki and Dilov, 2005; Schlagenhauf et al., 2008) and theoretically (e.g., Bürgmann et al., 1994; Cowie and Scholz, 1992b; Davatzes and Aydin, 2003; Du and Aydin, 1995; Martel, 1997; Mutlu and Pollard, 2008; Segall and Pollard, 1983; Willson et al., 2007). Faults may grow in width until they break the entire brittle layer (e.g., Mansfield and Cartwright, 2001). More commonly, they grow in length, either bilaterally or unilaterally, so that the fault plane expands horizontally. The along-strike growth is referred to as "horizontal or lateral propagation" (e.g., Keller et al., 1999; Manighetti et al., 2001a). The horizontal fault lengthening may occur at fast rates, up to several cm/year (e.g., Armijo et al., 1999; Bennett et al., 2006; Childs et al., 2003; Hubert-Ferrari et al., 2003; Keller et al., 1999; Manighetti et al., 1997, 1998, 2001b; Meyer et al., 1998; Morewood and Roberts, 1999; Mueller and Talling, 1997). While evidence for fault growth and especially horizontal propagation are clear, the actual growth processes are difficult to document and therefore are not fully understood. Yet, it is important to understand these processes: as a fault extends, it breaks and hence damages the material more. Meanwhile, it gets an increased ability to interact with other faults, and these interactions may lead to break the material even more.

* Corresponding author.
E-mail address: manighetti@geoazur.unice.fr (I. Manighetti).

http://dx.doi.org/10.1016/j.crte.2015.05.002
1631-0713/

To understand how natural faults are growing, a first step is to determine in which direction(s) they have propagated over their lifetime (i.e., generally several 10^4–10^6 year, later referred to as "long-term"). For large-scale faults that cut through the entire brittle crust (i.e. fault length $L_f \sim$ several 10 km), the direction(s) of long-term lengthening can be inferred from dating offsets along the fault (Table S1 in Supplementary material and references therein). Yet such dating is difficult, and therefore the direction(s) of long-term propagation is (are) rarely known for large-scale faults. Fault growth and propagation have thus been mostly studied at small scale, mainly in laboratory experiments. A common finding is that faults subjected to mixed normal and shear loads, as most natural faults are, develop off-fault splay fractures and faults at and around the propagating tip(s) of the parent fault (e.g., Brace and Bombolakis, 1963; Moore and Lockner, 1995; Nemat-Nasser and Horii, 1982; Otsuki and Dilov, 2005; Reches and Lockner, 1994). Furthermore, the geometries of experimental splay fault networks are similar to the geometries of splay fractures and faults observed at the tips of macroscopic natural faults (e.g., Granier, 1985; McGrath and Davison, 1995). This similarity has led some authors to suggest that:

(i) splay fault networks might be a general phenomenon developed on all types of parent faults and in different materials (e.g., Granier, 1985; McGrath and Davison, 1995);
(ii) splay fault networks might be used to track the propagation direction of a parent fault (e.g., Kim et al., 2003; McGrath and Davison, 1995; Manighetti et al., 1997, 1998; Vermilye and Scholz, 1998).

Our objective is to examine whether the suggestions above are valid, and to define the scales they might apply to. We analyze a worldwide population of crustal faults whose direction(s) of long-term propagation has (have) been documented. The faults span a broad range of lengths (from 10^{-5} to 10^3 km), and are of all slip modes. On published fault maps, we identify the parent fault trace and the secondary faults off the parent fault. We show the systematic development of secondary off-fault splay networks at the propagating tips of the parent faults. We establish scaling relations that reveal the genetic and generic link between parents and tip splay faults and that provide quantitative constraints on the width and length of damage zones around faults.

2. Off-fault splay networks at propagating fault tips

The term "splay fault" commonly refers to subsidiary faults that branch off a main fault and form an acute angle to that fault (Fig. 1; e.g., Davatzes and Aydin, 2003; Granier, 1985; McGrath and Davison, 1995). Although more restrictive definitions have been suggested (Ando et al., 2009; Scholz et al., 2010), here we use that simple definition. Note that splay faults have also been referred as wing cracks, horsetails, branch faults, bifurcating faults, etc. (e.g., Davatzes and Aydin, 2003; d'Alessio and Martel, 2004; de Joussineau et al., 2007; Granier, 1985; McGrath and Davison, 1995).

When referring to "long-term fault propagation", we refer to the fault lengthening over the whole or a long part of the fault history. Most of the faults we analyze are long-lived features with a lifetime of several 10^4–10^6 year. It is possible that, over such a long lifetime, a fault goes through phases when it does not propagate laterally but rather accumulates displacement at a constant length (see "Discussion"). Even so, the fault lengthens overall in one or two directions over its whole history, and this is the overall lengthening that we consider here.

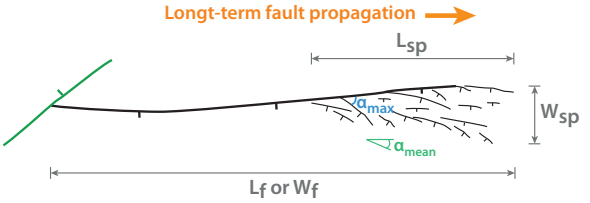

Fig. 1. (Color online.) Schematic map-view representation of a fault with off-fault tip splays. The parent fault trace (here, a normal fault) is represented with a thick line and the splay faults with thin traces. In accordance with results discussed in present study, tip splays are developed at the propagating parent fault's tip, whereas no splay is observed at the non-propagating fault tip (here, intersection with an oblique nearby fault, in green). L_f is the parent fault's length, L_{sp} and W_{sp} are the length and width of the tip splay network, respectively, α_{mean} and α_{max} are the mean and maximum angles, respectively, between splays and parent fault.

We analyze a population of 47 crustal faults worldwide, which have been mapped in prior works and whose direction(s) of long-term propagation has (have) been documented (Table S1 and references therein). The latter condition is the one that most limits the dataset. Five example fault maps are shown in Fig. 2 (all fault maps are shown in Fig. ES I in supplementary material). The population includes 23 normal, 3 reverse, and 21 strike-slip faults. Ninety-one percent of the faults were mapped in the horizontal plane, and this allows examining those faults along their length (L_f, Table S1 and Fig. ES I). The remaining $\sim$9% were observed in cross-section, and therefore, we examine these faults along their top-to-bottom width (W_f, Table S1 and Fig. ES I). The faults have a broad range of sizes (L_f or W_f) ranging from 10^{-5} to 2300 km. About half of the faults have a length greater than twice a standard seismogenic thickness (i.e., $L_f > \sim 40$ km), and hence are expected to cut through the entire crust.

The fault maps were originally done at different scales and resolutions, and thus provide different levels of detail (Fig. 2 and Fig. ES I). Yet, in all published maps, the parent fault trace is well identified (in red in Fig. 2 and Fig. ES I), whereas the secondary faults off the parent trace are clearly discriminated (see below). We have redrawn the fault maps to provide a comprehensive vision of the entire fault zones, but we have not modified the original mapping.

Faults are commonly flanked with secondary faults that branch off at intervals along their length (Fig. ES I). These along-strike subsidiary faults might be relicts of prior stages of the parent fault evolution (e.g., d'Alessio and Martel, 2004; de Joussineau and Aydin, 2007). We focus on the splay networks closest to the fault tips since they are expected to be the youngest (e.g., de Joussineau and Aydin, 2007), and hence those to still show their original geometry. We call them the "fault tip splays" (in orange in Fig. 2 and Fig. ES I). In most fault cases, the discrimination of fault tip splays from other off-fault

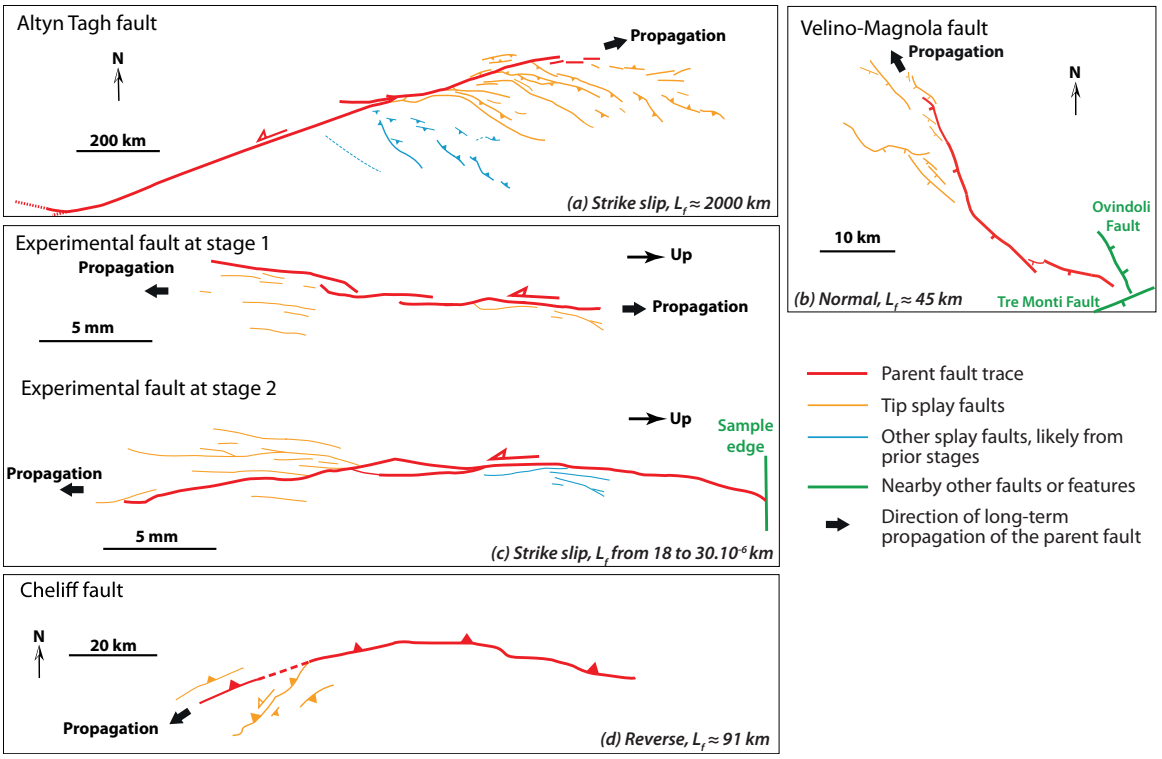

Fig. 2. (Color online.) Five example fault maps analyzed in the present study (from Fig. ES I in Supplementary material where all 47 fault maps are shown). The maps are redrawn from their original versions to discriminate the parent (in red) and the tip splay faults (in orange). In blue are splay faults that likely formed in earlier stages of fault growth. In green are nearby faults or features. The direction of long-term propagation of the parent faults, documented in Table S1, is indicated with a black arrow. L_f is the parent fault's length. (a) Altyn Tagh strike-slip fault (Meyer et al., 1998; Tapponnier et al., 2001); (b) Velino-Magnola normal fault (Schlagenhauf et al., 2011); (c) two stages of growth of an experimental strike-slip fault (Otsuki and Dilov, 2005); (d) Cheliff reverse fault (Boudiaf et al., 1998; Yielding et al., 1989).

features is straightforward as a significant distance separates them (for example, see Fig. 2c). In other cases, the fault tip splays are observed to emanate from a pronounced bend or a step-over in the parent fault trace, and this specific origin allows their discrimination (for example, see Fig. 2a).

The direction of long-term propagation of the parent faults was inferred from different evidences (Table S1 and references therein). For the three experimental faults in the population, the along-strike propagation was directly observed (Fig. 2c). For a number of other faults, the direction of long-term lengthening was inferred from the dating of offset or deformed features along the fault, which revealed the age decrease of the fault along its length. On other faults, the cumulative displacement was shown to progressively decrease along the fault length, as expected along a propagating fault whose age follows an along-strike decrease. Similarly, a significant along-strike decrease of the long-term fault slip rate suggests that the fault becomes younger in the direction of apparent slowing, and this criterion was also used in a few cases (Table S1). In other cases, the fault segment(s) closest to the actual fault tip were shown to be younger than the rest of the fault.

On all of the 47 fault maps, fault tip splays are observed to extend near the propagating parent fault tips (Fig. 2 and Fig. ES I). The splay faults generally form acute angles with the primary fault when the latter is observed in the direction of propagation (angles discussed in next section). The tip splay networks show a similar, tree-like or cone-shaped geometry, widening away from the propagating parent fault tip. In most cases, the splays are developed on one side only of the parent fault, but networks more symmetric about the primary fault exist in a few cases. Generally, the splays extend both ahead of the parent fault tip and around a significant fraction of the fault length behind the fault tip (Figs. 1 and 2 and Fig. ES I). The geometric patterns of the tip splays are similar for all parent fault slip modes. On strike-slip (or shear) faults, splays most commonly develop on one side of the parent fault only (yet symmetric networks also exist, for example, see Figs. ES I-4), but this side is either the extensive (for example, see Fig. ES I-5) or the compressive quadrant (for example, see Fig. 2a) of the shear fault. On normal faults, the tip splays most commonly develop in the parent fault hanging wall, but in a few cases, they form in the footwall (for example, see Fig. ES I-18) or in both fault compartments (for example, see Fig. ES I-38). On reverse faults, tip splays are most commonly developed in the hanging wall, but data are too scarce to be conclusive.

Because the degree of detail is different from one map to another, the data in Fig. 2 and Fig. ES I do not allow discussing the length and slip mode of the individual splay faults. We can only state that, in all cases, the tip splay networks include faults of different sizes, some of them

having a length of the same order as that of the parent fault. In many cases, independently of the parent fault slip mode, the splay faults seem to have a dominant dip-slip component. Yet strike-slip splay faults are also observed around the propagating tips of strike-slip parent faults (for example, see Fig. ES I-13).

About 80% of the faults seem to have mainly propagated unilaterally over their lifetime (Table S1). In contrast with their propagating tips, no splay network is observed at their non-propagating end (Table S1, Fig. 2 and Fig. ES I). Instead, the faults commonly terminate there by abutting another, markedly oblique fault of similar or different slip mode (Figs. 1 and 2b), or by stepping to a distant, roughly parallel fault with a similar slip mode (for example, see Fig. ES I-6).

We thus conclude that, regardless of their slip mode, of their length, of their geological context, and of their history, faults have their propagating tip(s) flanked or surrounded by a network of oblique, secondary splay faults. The tip splay networks have a significant size, and a similar tree-like geometry widening in the direction of long-term propagation (Fig. 1).

3. Scaling relations between off-fault tip splays and parent faults

We now examine the size properties of the tip splay networks with respect to the parent fault size. On each of the fault maps, we have measured the length (L_{sp}, measured parallel to the parent fault) and the width (W_{sp}) of the fault tip splay network(s), along with the mean (α_{mean}) and maximum (α_{max}) angles that the tip splay faults form with their parent fault (Figs. 1 and 2, Fig. ES I and Table S2). We report these quantities to the parent fault length (L_f), measured parallel to the mean fault strike and made to include the splay network(s). W_{sp} is the greatest width of a splay zone, measured perpendicular to the parent fault trace (i.e., W_{sp} is measured in the horizontal plane for 91% of the faults, and in the vertical plane for the other few faults). The angles α_{mean} and α_{max} are measured with respect to the mean strike of the parent fault (Fig. 1).

Because the fault maps have different resolutions, the measurements cannot be made with a great precision, and uncertainties cannot be properly quantified. Yet, the order of magnitude is all that is important to examine general scaling relations between the various quantities, especially when log scales are used, as we do below.

We first examine the length of the tip splay networks, L_{sp}, with respect to the length of the parent faults, L_f (Fig. 3). Although the data show some variability, they reveal a consistent trend throughout the entire range of length scales, showing that the length of the splay networks at the propagating fault tips increases with the length of the parent fault (Fig. 3a). The best-fit function to the data is a power law with an exponent of ~ 1 (Fig. ES IIa). The data can thus be best represented with a more realistic linear function with zero intercept: $L_{sp} = 0.34\, L_f$ (Fig. 3a). Therefore, the length of a tip splay network at a propagating fault tip is about one third of the parent fault length. This scaling relation is independent of the parent fault slip mode. A similar linear relation is indeed found for the strike-slip faults alone ($L_{sp} = 0.30\, L_f$, Fig. 3b), the normal faults alone

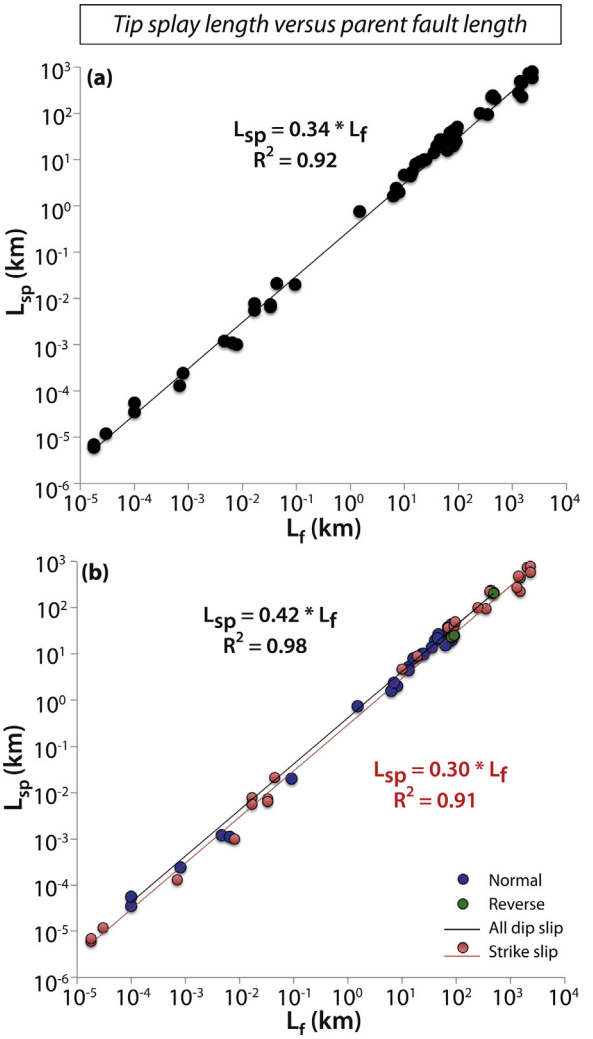

Fig. 3. (Color online.) Scaling relation between parent- and tip splay-fault lengths (data from Fig. ES I and Table S2 in Supplementary material). L_f is the parent fault's length, L_{sp} is the length of the tip splay network at the propagating parent fault's tip. (a) For the entire fault population. The black line is the best-fitting linear regression whose equation is indicated on the graph. (b) For the entire fault population discriminated from fault slip mode (colored symbols). The black and the red lines are the best-fitting linear regressions for the dip-slip and the strike-slip fault data, respectively, whose equations are indicated on the graph. See Fig. ES IIa–b for power law fits to the data, and Fig. ES IIIa for specific analysis of normal fault data.

($L_{sp} = 0.40\, L_f$, Fig. ES IIIa), and the dip-slip faults together ($L_{sp} = 0.42\, L_f$, Fig. 3b; reverse faults are too few to be examined alone) (see Figs. ES IIb and ES IIIa for power law functions).

We then examine the width of the tip splay networks, W_{sp}, with respect to L_f (Fig. 4). As before, although the data show some variability, they reveal a consistent trend throughout the entire range of length scales, which shows that the width of the tip splay networks at the propagating fault tips increases with the length of the parent fault (Fig. 4a). The best-fit function to the data is a power law with an exponent of ~ 1 (Fig. ES IIc). The data can thus be best represented with a more realistic linear function with zero intercept: $W_{sp} \sim 0.09\, L_f$ (Fig. 4a). Therefore, the width

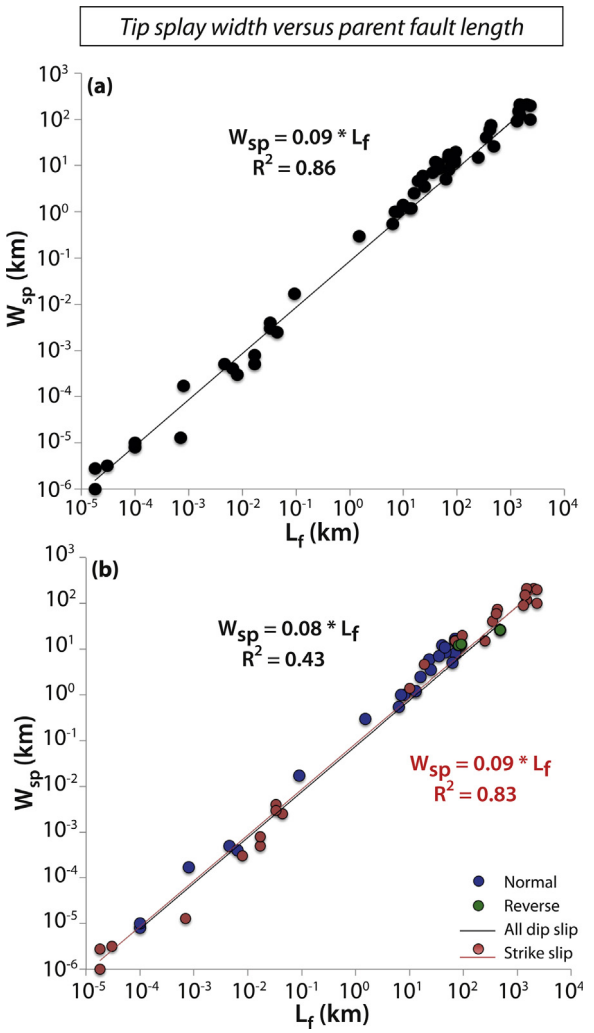

Fig. 4. (Color online.) Scaling relation between parent fault length and width of tip splay network (data from Fig. ES I and Table S2). L_f is the parent fault's length, W_{sp} is the width of the tip splay network at the propagating parent fault's tip. (a) For the entire fault population. The black line is the best-fitting linear regression whose equation is indicated on the graph. (b) For the entire fault population discriminated from fault slip mode (colored symbols). The black and the red lines are the best-fitting linear regressions for the dip-slip and the strike-slip fault data, respectively, whose equations are indicated on the graph. See Fig. ES IIc–d for power law fits to the data, and Fig. ES IIIb for specific analysis of normal fault data.

of a tip splay network at a propagating fault tip is about a tenth of the parent fault length. A similar linear relation is found for the strike-slip faults alone ($W_{sp} = 0.09\,L_f$, Fig. 4b), the normal faults alone ($W_{sp} \sim 0.18\,L_f$, Fig. ES IIIb), and the dip-slip faults together ($W_{sp} \sim 0.08\,L_f$, Fig. 4b) (see Fig. ES IId and ES IIIb for power law functions). Note that, for dip-slip faults, the linear fit with zero intercept is fairly poor ($R^2 = 0.43$, Fig. 4b); a power law fit is significantly better ($R^2 = 0.99$, Fig. ES IId), but provides a similar result: $W_{sp} = 0.13\,L_f$.

The scaling relations above keep similar whether the parent faults cut through, or not, the entire crust (Fig. ES IV).

Finally, we examine the angle relationships between the parent and the splay faults (Fig. 1). The maximum angles between splays and parent faults range between a few degrees and $\sim 90°$ (Fig. 5a), yet peak at 30–50°. The distribution of mean angles shows two peaks, at about 10–20° and 30–40°, and a threshold at $\sim 50°$ (Fig. 5b). Almost half of the splay networks trends at an average angle of 10–20° to their parent fault strike. We note that this measured mean angle is consistent with the mean angle one might infer from the two scaling relations described above (tan $(\alpha_{mean}) = W_{sp}/L_{sp}$ and hence tan $(\alpha_{mean}) = (0.09\,L_f)/(0.34\,L_f)$, which yields $\alpha_{mean} \sim 15°$).

4. Discussion

We have shown that off-fault splay networks are found systematically at propagating fault tips, whereas they are absent at non-propagating fault ends. This applies to the broad range of parent fault lengths that we have examined, and for parent faults being normal, reverse or strike-slip. Furthermore, the fault tip splay networks show a similar overall shape, resembling a fan widening in the direction of the parent fault long-term propagation. These observations suggest together that tip splay networks are genetically linked to the along-strike (or along-width) growth of their parent faults over the long term. We

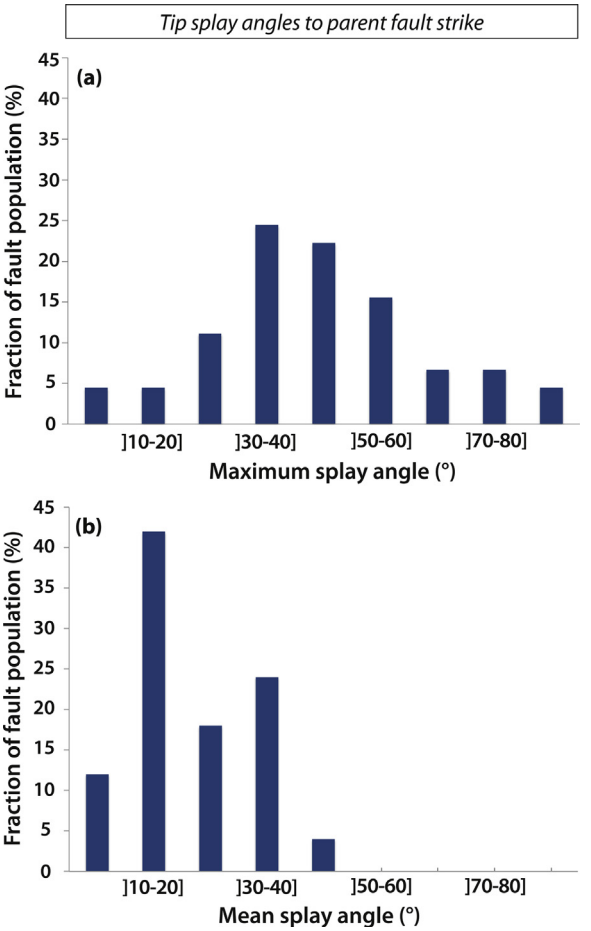

Fig. 5. (Color online.) Distribution of (a) maximum and (b) mean splay fault angles relative to average parent fault strike (data from Fig. ES I and Table 2). See Fig. 1 for angle definition.

determine scaling relations that additionally show that both the length and the width of the tip splay networks are a systematic, similar fraction of the parent fault length (~ 0.3 and ~ 0.1, respectively). The mean angles of the splays to their parent faults are also systematically in the same narrow range (10–20° for the majority, $< 50°$ in all cases). Therefore, off-fault tip splay networks are a genetic and a generic property of faults, indicative of their long-term propagation. The sizes of the splay networks and their geometrical relations with the parent faults are self-similar, independent of the length, slip mode, history, and context of the primary faults.

Some of the results above have been suggested in earlier works, yet from more limited data. In particular, the fan-shaped arrangement of the tip splay networks has been described on small natural faults (i.e., L_f 10^{-3}–10^{2} m; e.g., Davatzes and Aydin, 2003; de Joussineau and Aydin, 2007; Granier, 1985; McGrath and Davison, 1995; Kim et al., 2003; Segall and Pollard, 1983), and on experimental and numerical faults or cracks (e.g., Aranson et al., 2000; Marder and Fineberg, 1996; Mutlu and Pollard, 2008; Otsuki and Dilov, 2005). The genetic relation between off-fault splays and propagation of parent faults has been suggested for a few natural faults (e.g., Ellis and Dunlap, 1988; Kim et al., 2003; Manighetti et al., 1997, 1998, 2001b; McGrath and Davison, 1995; Vermilye and Scholz, 1998; Wu and Bruhn, 1994), and from experiments and theoretical models (e.g., Aranson et al., 2000; Davatzes and Aydin, 2003; Du and Aydin, 1995; Martel, 1997; Moore and Lockner, 1995; Mutlu and Pollard, 2008; Segall and Pollard, 1983; Willemse and Pollard, 1998). Angular relations between splay and parent faults have also been studied on natural and experimental faults, generally of small scales. Although the definition of splays slightly varies among studies (see discussion in Scholz et al., 2010), splays are found to form acute angles to parent faults, generally $< 50°$ and most commonly in the range 10–30° (Ando et al., 2009; Cooke, 1997; Davatzes and Aydin, 2003; d'Alessio and Martel, 2004; de Joussineau et al., 2007; Granier, 1985; Martel, 1997; McGrath and Davison, 1995; Moore and Lockner, 1995; Reches and Lockner, 1994; Segall and Pollard, 1983; Willemse and Pollard, 1998), with peak values at 17–19° (Ando et al., 2009; de Joussineau et al., 2007). By contrast, the length and width of splay zones have not been much discussed in the literature. From theoretical models or limited observations, it has been suggested, however, that the length (e.g., Bürgmann et al., 1994; de Joussineau et al., 2007; Kim et al., 2003; McGrath and Davison, 1995) and the width (e.g., Davatzes and Aydin, 2003; de Joussineau et al., 2007, Vermilye and Scholz, 1998) of splay zones might scale with parent fault lengths or total displacements. The length-to-length, and width-to-length ratios that were suggested are in the range 0.2–0.6 (de Joussineau et al., 2007), and 0.016–0.2 (de Joussineau et al., 2007; Vermilye and Scholz, 1998), respectively. Therefore, our results are consistent with those from the few prior studies. Yet, since they are based on a much larger dataset spanning a broader range of scales from millimetres to thousands of kilometres, they generalize the prior observations and they demonstrate the generic, self-similar properties of the tip splay networks.

Differences also exist between our observations and those from prior studies. The common vision of splays is that they develop mainly on strike-slip faults (e.g., de Joussineau et al., 2007; Friedman and Logan, 1970; Granier, 1985; Kim et al., 2003; Martel, 1990; Mutlu and Pollard, 2008; Petit and Barquins, 1988; Rispoli, 1981; Segall and Pollard, 1983), they are mostly made of extensional features (e.g., Cooke, 1997; de Joussineau et al., 2007; Reches and Lockner, 1994), and they form in the extensive quadrants of the parent faults (e.g., Cooke, 1997; Granier, 1985; Mutlu and Pollard, 2008). Rather, we find that tip splays form on all faults, normal, reverse and strike-slip (as observed by McGrath and Davison, 1995), they include second-order faults that can be normal, reverse or strike-slip (Fig. ES I, see also McGrath and Davison, 1995), and they develop in either extensional or compressional quadrants, sometimes in both (as observed by Willemse and Pollard, 1998; Fig. ES I).

Tip splay faults have been interpreted to form as a response to the large stress concentrations, especially tensile stresses, that exist at fault terminations (e.g., Cooke, 1997; Cotterell and Rice, 1980; Du and Aydin, 1995; Nemat-Nasser and Horii, 1982; Rispoli, 1981; Segall and Pollard, 1983; Vermilye and Scholz, 1998, 1999; Willemse and Pollard, 1998; Willson et al., 2007). The amount and distribution of stresses at fault ends depend on several factors, including the fault slip mode, the displacement gradients at fault tips, the variability of fault friction, the mechanical behavior of the host rocks near the fault tips (e.g., Bürgmann et al., 1994; Cooke, 1997). The finding of tip splay networks having generic properties independent of parent fault scale, slip mode, context, etc., suggests that either the parent fault tip stress field does not play a dominant role in the formation of the tip splay faults, or the parent fault tip stress field also has generic properties independent of parent fault scale, slip mode, context, etc. Ando et al. (2009) and Scholz et al. (2010) favor the former hypothesis and suggest that the formation of at least the largest splays is driven by regional stresses, not by stress concentrations at parent fault tips. A number of authors have actually suggested that splays might form parallel to the maximum regional compressive stress (e.g., Du and Aydin, 1995; McGrath and Davison, 1995; Mutlu and Pollard, 2008; Segall and Pollard, 1983; Vermilye and Scholz, 1998). Yet the finding that tip splay networks have self-similar geometrical properties make it unlikely that they emerge from variable, site-dependent, regional stress fields. Therefore, we favor the latter hypothesis, and suggest that self-similar tip splay networks form as a response to self-similar parent fault tip stress distributions.

It has been shown that distributions of cumulative displacements along faults have a generic overall shape, which is basically triangular and generally asymmetric whatever the fault size, slip mode, context, etc. (e.g., Manighetti et al., 2001a, 2009, 2015; Martel and Shacat, 2006; Muraoka and Kamata, 1983; Nicol et al., 2005; Peacock and Sanderson, 1996; Scholz and Lawler, 2004; Soliva and Benedicto, 2004, for normal faults; e.g., Bürgmann et al., 1994; Farbod et al., 2011; McGrath and Davison, 1995; Pachell and Evans, 2002; Peacock, 1991, for strike-slip faults; e.g., Davis et al., 2005; Ellis and Dunlap,

1988; Shaw et al., 2002, for reverse faults). Furthermore, the displacement-length profiles have been shown to taper in the direction of long-term fault propagation (e.g., Davis et al., 2005; Manighetti et al., 2001a). Because static stress on fault planes is basically inversely proportional to cumulative displacement, static stress must gradually vary along faults, from being minimal in the zone of maximum cumulative displacement to being highest at the other fault end where displacement tapers to zero. Therefore, on-fault static stress must gradually increase in the direction of parent fault propagation (Manighetti et al., 2015). Because the envelope shape of displacement-length distributions is generic, along fault static stress gradients must also be. To reconcile the on-fault stress variability with the fairly linear scaling relation that is observed for all faults between their maximum displacement and their length (references in introduction), it has been suggested that the excess on-fault stresses that result from the gradual displacement decrease along the fault, are diffused off the fault, in the host rocks, where they produce microscopic and macroscopic "damage" fractures, faults and possibly other types of deformation (e.g., Cooke, 1997; Granier, 1985; Manighetti et al., 2004; Scholz and Lawler, 2004). Off-fault stress and strain diffusion might dominantly occur during repeated earthquakes on a fault (e.g., Cappa et al., 2014 and references therein; Manighetti et al., 2005). Yet, although damage might be created dynamically during earthquake events, part of the coseismic deformation is irreversible and thus accumulates over time to produce permanent deformation. We suggest that the observed splay faults are part of the macroscopic, cumulative damage features that progressively form around a parent fault in response to repeated episodes of coseismic stress and strain diffusion. We pointed out that splay networks are not seen at fault tips that no longer propagate (due to arrest at a barrier or step to another fault; e.g., d'Alessio and Martel, 2004; Manighetti et al., 2001a, 2004). This might be because accumulated on-fault displacements are greatest at arrested fault ends (Manighetti et al., 2001a) and therefore, off-fault stress and strain dissipation is minimal at these non-propagating tips.

Observations of damage zones in natural fault cases, experiments and theoretical models concur to show that damage zones migrate with the propagating fault tip (e.g., de Joussineau and Aydin, 2007; Faulkner et al., 2011; Manighetti et al., 2004; Otsuki and Dilov, 2005, Fig. 2c). Consequently, a propagating fault has its trace eventually flanked by a wake of off-fault damage fractures and faults, and hence by a wake of splay faults. Here, we have focused on the splay faults closest to the present propagating fault tips. These tip splay networks are thus expected to be the most recent damage zone formed during the most recent episode of fault lengthening. The scaling relation we found between parent fault length and width of tip splay networks implies that damage zones enlarge as the parent fault length increases. This proportional growth explains why tip splay networks, and more generally damage zones have a wedge shape broadening in the direction of long-term fault propagation. Because tip splay networks are the most recent damage zones, their constitutive splay faults are inherently immature, and are independent of the lifetime of their parent fault. This may explain why the geometric properties of tip splay networks are similar for faults with different histories.

The way faults lengthen over time is unclear. It seems that faults grow over the long term through alternating phases of dominant displacement accumulation, possibly at constant length, and of dominant lateral propagation, possibly with little displacement increase (e.g., Bull et al., 2006; Childs et al., 2003; Giba et al., 2012; Manighetti et al., 2015; Nicol et al., 2005, 2010; Schlagenhauf et al., 2008). The times of displacement accumulation at fairly constant length can be long, up to several 10^4–10^6 year (e.g., Bull et al., 2006; Nicol et al., 2005). During these long phases, off-fault stresses build up around the fault, and thus contribute to enhance the growth of the damage splay faults, both ahead and around the parent fault tips. It is likely that, at some stage, some of the splay faults might be large enough to coalesce with the parent fault, which, consequently, becomes longer (e.g., Manighetti et al., 2015). In their experimental work, Moore and Lockner (1995) show that, furthermore, the uneven distribution of the damage cracks tends to pull the propagating fault tip slightly away from the overall fault strike (as observed in Fig. 2c). As a result, the fault steps laterally before it resumes propagating parallel to its mean strike. Damage splay faults might thus contribute to both fault lengthening and fault segmentation (formation of step-overs).

The theoretical models suggest that splay faults may develop on a significant section of a fault behind its tip, provided that there exist spatial gradients in on-fault stresses and/or changes in frictional strength along that fault section (e.g., Bürgmann et al., 1994; Cooke, 1997). The fault section with varying stress and friction is referred to as the fault cohesive end zone, whereas off-fault deformation is described as the process zone (e.g., Cowie and Scholz, 1992b; Scholz et al., 1993). Up to now, the cohesive end zone and the process zone have been supposed to be of small size compared to the parent fault length. In the framework of these theoretical models, the fault sections that we observe to be flanked with tip splay networks would be the cohesive end zones, whereas the tip splay networks would be the process zones. Yet, contrary to the common vision, both are found to be of large scale, with a ratio of the cohesive end zone length to the fault length of ~ 0.3, and a ratio of the process zone width to the fault length of ~ 0.1.

A growing body of evidence suggests that, during an earthquake, a significant fraction of the coseismic slip is dissipated off the main rupture plane into the permanent damage zone that surrounds the fault (e.g., Cappa et al., 2014 and references therein). We have shown that the long-term damage zone has a maximum width of $\sim 10\%$ of the parent fault length. We thus infer that coseismic dissipation might occur away from a rupture zone as far as a distance of 10% of the total fault length (that distance is a maximum, of concern only when the entire fault length is broken). This suggests that coseismic deformations and stress transfers might be significant in broad regions about a principal rupture trace, up to 5 km for a 50-km-long fault that would be entirely broken, and up to several tens of kilometres for broken faults longer than 200 km.

5. Conclusions

From the analysis of a dense population of faults with variable lengths (from millimetres to thousands of kilometres) and slip modes (normal, reverse, and strike-slip), we have shown that secondary off-fault tip splay networks are a genetic and a generic property of faults indicative of their long-term propagation. Oblique tip splay networks form adjacent to any propagating parent fault tip, and therefore their identification is a robust evidence of the long-term propagation of a fault. We propose that tip splay networks are parts of the damage zones that develop off a fault at intervals along its trace as the fault grows in space and time. The tip splays would form the most recent damage zone.

Additionally, the tip splay networks have self-similar geometrical relations with the parent fault. Their length and width are about a third and a tenth, respectively, of the parent fault length, whereas tip splay faults commonly form a 10–20° acute angle with the parent fault. These scaling relations suggest that elastic properties of host rocks might be modified at large distances away from a fault, up to 10% of the fault length. Furthermore, the similarity of tip splay networks from ranges of millimetres to thousands of kilometres and for all slip modes suggests that splay faults might form similarly at even larger scales, such as those concerned with continental rift and oceanic ridge propagation, or propagation of giant plate boundary faults (e.g., Hubert-Ferrari et al., 2003).

An increasing literature describes splay faults in subduction zones, adjacent to the upper tip of the plate interface (Fig. ES V in supplementary material). It is commonly thought that these splay faults are responsible, at least partly, for tsunami generation during large subduction earthquakes (e.g., Moore et al., 2007). We suggest that the subduction splay faults might form in a similar manner to the continental splays that we have described here, the parent fault length being the width of the seismogenic zone (W_f). If so, we expect that subduction splay faults might develop over long sections of the subduction interface ($\sim$30% of W_f) and extend over distances up to 10% of W_f (Fig. ES V). If these suggestions are verified, they might provide a guide to anticipate the extent of the zones where tsunamigenic faults might be looked for.

Acknowledgments

This work has been done in tribute to our beloved colleague and friend Jean-François Stéphan. All the data that are used are available in the literature. This paper has been reviewed by Chief Editor Vincent Courtillot and by Jérôme Van der Woerd.

Appendix A. Supplementary data

Supplementary data associated with this article can be found, in the online version, at http://dx.doi.org/10.1016/j.crte.2015.05.002.

References

Ando, R., Shaw, B.E., Scholz, C.H., 2009. Quantifying natural fault geometry: statistics of splay fault angles. Bull. Seismol. Soc. Am. 99 (1), 389–395.
Aranson, I.S., Kalatsky, V.A., Vinokur, V.M., 2000. Continuum field description of crack propagation. Phys. Rev. Lett. 85 (1), 118–121.
Armijo, R., Meyer, B., Hubert, A., Barka, A., 1999. Westward propagation of the North Anatolian fault into the northern Aegean: timing and kinematics. Geology 27 (3), 267–270.
Bennett, E., Youngson, J., Jackson, J., Norris, R., Raisbeck, G., Yiou, F., 2006. Combining geomorphic observations with in situ cosmogenic isotope measurements to study anticline growth and fault propagation in Central Otagon, New Zealand. New Zeal. J. Geol. Geophys. 49 (2), 217–231.
Boudiaf, A., Ritz, J.F., Philip, H., 1998. Drainage diversions as evidence of propagating active faults: example of the El Asnam and Thenia faults, Algeria. Terra Nova-Oxford 10 (5), 236–244.
Brace, W.D., Bombolakis, E.G., 1963. A note on brittle crack growth in compression. J. Geophys. Res. 68 (12), 3709–3713.
Bull, J.M., Barnes, P.M., Lamarche, G., Sanderson, D.J., Cowie, P.A., Taylor, S.K., Dix, J.K., 2006. High-resolution record of displacement accumulation on an active normal fault: implications for models of slip accumulation during repeated earthquakes. J. Struct. Geol. 28 (7), 1146–1166.
Bürgmann, R., Pollard, D.D., Martel, S.J., 1994. Slip distributions on faults: effects of stress gradients, inelastic deformation, heterogeneous host-rock stiffness, and fault interaction. J. Struct. Geol. 16 (12), 1675–1690.
Cappa, F., Perrin, C., Manighetti, I., Delor, E., 2014. Off-fault long-term damage: a condition to account for generic, triangular earthquake slip profiles. Geochem. Geophys. Geosyst. 15 (4), 1476–1493.
Cartwright, J.A., Trudgill, B.D., Mansfield, C.S., 1995. Fault growth by segment linkage: an explanation for scatter in maximum displacement and trace length data from the Canyonlands Grabens of SE Utah. J. Struct. Geol. 17 (9), 1319–1326.
Childs, C., Nicol, A., Walsh, J.J., Watterson, J., 2003. The growth and propagation of synsedimentary faults. J. Struct. Geol. 25 (4), 633–648.
Cooke, M.L., 1997. Fracture localization along faults with spatially varying friction. J. Geophys. Res. 102 (B10), 22425–22434, http://dx.doi.org/10.1029/97JB01829.
Cotterell, B., Rice, J., 1980. Slightly curved or kinked cracks. Int. J. Fracture 16 (2), 155–169.
Cowie, P.A., Scholz, C.H., 1992a. Displacement-length scaling relationship for faults: data synthesis and discussion. J. Struct. Geol. 14 (10), 1149–1156.
Cowie, P.A., Scholz, C.H., 1992b. Physical explanation for the displacement-length relationship of faults using a post-yield fracture mechanics model. J. Struct. Geol. 14 (10), 1133–1148.
d'Alessio, M.A., Martel, S.J., 2004. Fault terminations and barriers to fault growth. J. Struct. Geol. 26 (10), 1885–1896.
Davatzes, N.C., Aydin, A., 2003. The formation of conjugate normal fault systems in folded sandstone by sequential jointing and shearing, Waterpocket monocline. Utah. J. Geophys. Res. 108 (B10), ETG7.1–ETG7.15.
Dawers, N.H., Anders, M.H., Scholz, C.H., 1993. Growth of normal faults: displacement-length scaling. Geology 21 (12), 1107–1110.
Davis, K., Burbank, D.W., Fisher, D., Wallace, S., Nobes, D., 2005. Thrust-fault growth and segment linkage in the active Ostler fault zone, New Zealand. J. Struct. Geol. 27 (8), 1528–1546.
de Joussineau, G., Aydin, A., 2007. The evolution of the damage zone with fault growth in sandstone and its multiscale characteristics. J. Geophys. Res. 112, B12401.1–B12401.19, http://dx.doi.org/10.1029/2006jb004711.
de Joussineau, G., Mutlu, O., Aydin, A., Pollard, D.D., 2007. Characterization of strike-slip fault–splay relationships in sandstone. J. Struct. Geol. 29 (11), 1831–1842.
Du, Y., Aydin, A., 1995. Shear fracture patterns and connectivity at geometric complexities along strike-slip faults. J. Geophys. Res. 100 (B9), 18093–18102.
Ellis, M.A., Dunlap, W.J., 1988. Displacement variation along thrust faults: implications for the development of large faults. J. Struct. Geol. 10 (2), 183–192.
Farbod, Y., Bellier, O., Shabanian, E., Abbassi, M.R., 2011. Geomorphic and structural variations along the Doruneh Fault System (central Iran). Tectonics 30 (6), TC6014.1–TC6014.25.
Faulkner, D.R., Mitchell, T.M., Jensen, E., Cembrano, J., 2011. Scaling of fault damage zones with displacement and the implications for fault growth processes. J. Geophys. Res. 116 (B5), B05403.1–B05403.11.

Friedman, M., Logan, J.M., 1970. Microscopic feather fractures. Geol. Soc. Am. Bull. 81 (11), 3417–3420.
Giba, M., Walsh, J.J., Nicol, A., 2012. Segmentation and growth of an obliquely reactivated normal fault. J. Struct. Geol. 39, 253–267.
Granier, T., 1985. Origin, damping, and pattern of development of faults in granite. Tectonics 4 (7), 721–737.
Hubert-Ferrari, A., King, G., Manighetti, I., Armijo, R., Meyer, B., Tapponnier, P., 2003. Long-term elasticity in the continental lithosphere; modelling the Aden Ridge propagation and the Anatolian extrusion process. Geophys. J. Int. 153 (1), 111–132.
Jackson, J., Norris, R., Youngson, J., 1996. The structural evolution of active fault and fold systems in central Otago, New Zealand: evidence revealed by drainage patterns. J. Struct. Geol. 18 (2), 217–234.
Keller, E.A., Gurrola, L., Tierney, T.E., 1999. Geomorphic criteria to determine direction of lateral propagation of reverse faulting and folding. Geology 27 (6), 515–518.
Kim, Y.S., Peacock, D.C.P., Sanderson, D.J., 2003. Mesoscale strike-slip faults and damage zones at Marsalforn, Gozo Island, Malta. J. Struct. Geol. 25 (5), 793–812.
McGrath, A.G., Davison, I., 1995. Damage zone geometry around fault tips. J. Struct. Geol. 17 (7), 1011–1024.
Manighetti, I., Tapponnier, P., Courtillot, V., Gruszow, S., Gillot, P.Y., 1997. Propagation of rifting along the Arabia-Somalia plate boundary: the gulfs of Aden and Tadjoura. J. Geophys. Res. 102 (B2), 2681–2710.
Manighetti, I., Tapponnier, P., Gillot, P.Y., Jacques, E., Courtillot, V., Armijo, R., Ruegg, J.C., King, G., 1998. Propagation of rifting along the Arabia-Somalia plate boundary: into Afar. J. Geophys. Res. 103 (B3), 4947–4974.
Manighetti, I., King, G.C.P., Gaudemer, Y., Scholz, C.H., Doubre, C., 2001a. Slip accumulation and lateral propagation of active normal faults in Afar. J. Geophys. Res. 106 (B7), 13667–13696.
Manighetti, I., Tapponnier, P., Courtillot, V., Gallet, Y., Jacques, E., Gillot, P.Y., 2001b. Strain transfer between disconnected, propagating rifts in Afar. J. Geophys. Res. 106 (B7), 13613–13665.
Manighetti, I., King, G., Sammis, C.G., 2004. The role of off-fault damage in the evolution of normal faults. Earth Planet. Sci. Lett. 217 (3), 399–408.
Manighetti, I., Campillo, M., Sammis, C., Mai, P.M., King, G., 2005. Evidence for self-similar, triangular slip distributions on earthquakes: Implications for earthquake and fault mechanics. J. Geophys. Res. 110 (B5) .
Manighetti, I., Zigone, D., Campillo, M., Cotton, F., 2009. Self-similarity of the largest-scale segmentation of the faults: implications for earthquake behavior. Earth Planet. Sci. Lett. 288 (3), 370–381.
Manighetti, I., Caulet, C., Barros, L., Perrin, C., Cappa, F., Gaudemer, Y., 2015. Generic along-strike segmentation of Afar normal faults, East Africa: implications on fault growth and stress heterogeneity on seismogenic fault planes. Geochem. Geophys. Geosyst., http://dx.doi.org/10.1002/2014GC005691 (in press).
Mansfield, C., Cartwright, J., 2001. Fault growth by linkage: observations and implications from analogue models. J. Struct. Geol. 23 (5), 745–763.
Marder, M., Fineberg, J., 1996. How things break. Phys. Today 49 (9), 24–29.
Marrett, R., Allmendinger, R.W., 1990. Kinematic analysis of fault-slip data. J. Struct. Geol. 12 (8), 973–986.
Martel, S.J., 1990. Formation of compound strike-slip fault zones, Mount Abbot quadrangle, California. J. Struct. Geol. 12 (7), 869–882.
Martel, S.J., 1997. Effects of cohesive zones on small faults and implications for secondary fracturing and fault trace geometry. J. Struct. Geol. 19 (6), 835–847.
Martel, S.J., Shacat, C., 2006. Mechanics and interpretations of fault slip. AGU Geophys. Monogr. Ser. 170, 207–215.
Meyer, B., Tapponnier, P., Bourjot, L., Metivier, F., Gaudemer, Y., Peltzer, G., Shunmin, G., Zhitai, C., 1998. Crustal thickening in Gansu-Qinghai, lithospheric mantle subduction, and oblique, strike-slip controlled growth of the Tibet plateau. Geophys. J. Int. 135 (1), 1–47.
Moore, D.E., Lockner, D.A., 1995. The role of microcracking in shear-fracture propagation in granite. J. Struct. Geol. 17 (1), 95–114.
Moore, G.F., Bangs, N.L., Taira, A., Kuramoto, S., Pangborn, E., Tobin, H.J., 2007. Three-dimensional splay fault geometry and implications for tsunami generation. Science 318 (5853), 1128–1131.
Morewood, N.C., Roberts, G.P., 1999. Lateral propagation of the surface trace of the South Alkyonides normal fault segment, central Greece: its impact on models of fault growth and displacement–length relationships. J. Struct. Geol. 21 (6), 635–652.
Mueller, K., Talling, P., 1997. Geomorphic evidence for tear faults accommodating lateral propagation of an active fault-bend fold, Wheeler Ridge, California. J. Struct. Geol. 19 (3), 397–411.
Muraoka, H., Kamata, H., 1983. Displacement distribution along minor fault traces. J. Struct. Geol. 5 (5), 483–495.
Mutlu, O., Pollard, D.D., 2008. On the patterns of wing cracks along an outcrop scale flaw: a numerical modeling approach using complementarity. J. Geophys. Res. 113 (B6), B06403.1–B06403.20, http://dx.doi.org/10.1029/2007JB005284.
Nemat-Nasser, S., Horii, H., 1982. Compression-induced nonplanar crack extension with application to splitting, exfoliation, and rockburst. J. Geophys. Res. 87 (B8), 6805–6821.
Nicol, A., Walsh, J., Berryman, K., Nodder, S., 2005. Growth of a normal fault by the accumulation of slip over millions of years. J. Struct. Geol. 27 (2), 327–342.
Nicol, A., Walsh, J.J., Villamor, P., Seebeck, H., Berryman, K.R., 2010. Normal fault interactions, paleoearthquakes and growth in an active rift. J. Struct. Geol. 32 (8), 1101–1113.
Otsuki, K., Dilov, T., 2005. Evolution of hierarchical self-similar geometry of experimental fault zones: implications for seismic nucleation and earthquake size. J. Geophys. Res. 110 (B3), B03303.1–B03303.9.
Pachell, M.A., Evans, J.P., 2002. Growth, linkage, and termination processes of a 10-km-long strike-slip fault in jointed granite: the Gemini fault zone, Sierra Nevada, California. J. Struct. Geol. 24 (12), 1903–1924.
Peacock, D.C.P., 1991. Displacements and segment linkage in strike-slip fault zones. J. Struct. Geol. 13 (9), 1025–1035.
Peacock, D.C.P., Sanderson, D.J., 1996. Effects of propagation rate on displacement variations along faults. J. Struct. Geol. 18 (2), 311–320.
Petit, J.P., Barquins, M., 1988. Can natural faults propagate under mode II conditions? Tectonics 7 (6), 1243–1256.
Reches, Z.E., Lockner, D.A., 1994. Nucleation and growth of faults in brittle rocks. J. Geophys. Res. 99 (B9), 18159–18173.
Rispoli, R., 1981. Stress fields about strike-slip faults inferred from stylolites and tension gashes. Tectonophysics 75 (3), T29–T36.
Schlagenhauf, A., Manighetti, I., Malavieille, J., Dominguez, S., 2008. Incremental growth of normal faults: insights from a laser-equipped analog experiment. Earth Planet. Sci. Lett. 273 (3), 299–311.
Schlagenhauf, A., Manighetti, I., Benedetti, L., Gaudemer, Y., Finkel, R., Malavieille, J., Pou, K., 2011. Earthquake supercycles in central Italy, inferred from ^{36}Cl exposure dating. Earth Planet. Sci. Lett. 307 (3), 487–500.
Schlische, R.W., Young, S.S., Ackermann, R.V., Gupta, A., 1996. Geometry and scaling relations of a population of very small rift-related normal faults. Geology 24 (8), 683–686.
Scholz, C.H., Lawler, T.M., 2004. Slip tapers at the tips of faults and earthquake ruptures. Geophys. Res. Lett. 31 (21), L21609.1–L21609.4.
Scholz, C.H., Dawers, N.H., Yu, J.Z., Anders, M.H., Cowie, P.A., 1993. Fault growth and fault scaling laws: preliminary results. J. Geophys. Res. 98 (B12), 21951–21961.
Scholz, C.H., Ando, R., Shaw, B.E., 2010. The mechanics of first order splay faulting: the strike-slip case. J. Struct. Geol. 32 (1), 118–126.
Segall, P., Pollard, D.D., 1983. Nucleation and growth of strike slip faults in granite. J. Geophys. Res. 88 (B1), 555–568.
Shaw, J.H., Plesch, A., Dolan, J.F., Pratt, T.L., Fiore, P., 2002. Puente Hills blind-thrust system, Los Angeles, California. Bull. Seismol. Soc. Am. 92 (8), 2946–2960.
Soliva, R., Benedicto, A., 2004. A linkage criterion for segmented normal faults. J. Struct. Geol. 26 (12), 2251–2267.
Tapponnier, P., Ryerson, F.J., Van der Woerd, J., Mériaux, A.S., Lasserre, C., 2001. Long-term slip rates and characteristic slip: keys to active fault behaviour and earthquake hazard. C. R. Acad. Sci. Paris, Ser. IIa 333 (9), 483–494.
Vermilye, J.M., Scholz, C.H., 1998. The process zone: a microstructural view of fault growth. J. Geophys. Res. 103 (B6), 12223–12237.
Vermilye, J.M., Scholz, C.H., 1999. Fault propagation and segmentation: insight from the microstructural examination of a small fault. J. Struct. Geol. 21 (11), 1623–1636.
Walsh, J.J., Watterson, J., 1988. Analysis of the relationship between displacements and dimensions of faults. J. Struct. Geol. 10 (3), 239–247.
Willemse, E.J., Pollard, D.D., 1998. On the orientation and patterns of wing cracks and solution surfaces at the tips of a sliding flaw or fault. J. Geophys. Res. 103 (B2), 2427–2438.
Willson, J.P., Lunn, R.J., Shipton, Z.K., 2007. Simulating spatial and temporal evolution of multiple wing cracks around faults in crystalline basement rocks. J. Geophys. Res. 112 (B8), B08408.1–B08408.11.
Wu, D., Bruhn, R.L., 1994. Geometry and kinematics of active normal faults, South Oquirrh Mountains, Utah: implication for fault growth. J. Struct. Geol. 16 (8), 1061–1075.
Yielding, G., Ouyed, M., King, G.C.P., Hatzfeld, D., 1989. Active tectonics of the Algerian Atlas Mountains – evidence from aftershocks of the 1980 El Asnam earthquake. Geophys. J. Int. 99 (3), 761–788.